Supporting Information for "The Common Representative Intermediates Mechanism version 2 in the United Kingdom Chemistry and Aerosols Model"

S. Archer-Nicholls[1], N. L. Abraham[1,2], Y. M. Shin[1], J. Weber[1], M. R.

Russo[1,2], D. Lowe[3], S. Utembe[4], F. M. O'Connor[5], B. Kerridge[6,7],

B.Latter[6,7], R. Siddans[6,7], M. Jenkin[8], O. Wild[9], A. T. Archibald[1,2]

[1]Department of Chemistry, University of Cambridge, Cambridge, UK [2]National Centre for Atmospheric Science, Department of Chemistry, University of Cambridge, Cambridge, UK [3]University of Manchester, Manchester, UK [4]University of Melbourne, Melbourne, Australia [5]Met Office Hadley Centre, Exeter, UK [6]Remote Sensing Group, STFC Rutherford Appleton Laboratory, UK [7]NERC National Centre for Earth Observation, Leicester, UK [8]Atmospheric Chemistry Services, Okehampton, Devon, UK [9]Lancaster University, Lancaster, UK

Contents of this file

————

Corresponding author: A. T. Archibald, Department of Chemistry, University of Cambridge, Cambridge, UK. (ata27@cam.ac.uk)

November 23, 2020, 4:28pm

5. S5. Supporting Analysis of ozone

6. S6. Supporting Analysis of Nitrogen Containing Species

7. Figure S1. Difference in zonal mean $HONO_2$, NO_y, NO_x, NO_z and O_3 between StratTrop_NCon and StratTrop_Orig.

8. Figure S2. Comparison of selected inorganic bimolecular reaction rates in CRIv2 to equivalent reactions in StratTrop over an atmospherically relevant temperature range. Blue line is CRI rate, orange line StratTrop, both using scale on left axis, and black dot-dashed line shows ratio of CRI/StratTrop.

9. Figure S3. Comparison of inorganic bimolecular reaction rates in CRIv2 to equivalent reactions in StratTrop over an atmospherically relevant temperature range. Blue line is CRI rate, orange line StratTrop, both using scale on left axis, and black dot-dashed line shows ratio of CRI/StratTrop.

10. Figure S4. Comparison of selected organic bimolecular reaction rates in CRIv2 to equivalent reactions in StratTrop over an atmospherically relevant temperature range. Blue line is CRI rate, orange line StratTrop, both using scale on left axis, and black dot-dashed line shows ratio of CRI/StratTrop.

11. Figure S5. Ratios of selected termolecular reaction rate coefficients in CRIv2 to equivalent reactions in StratTrop over atmospherically relevant temperature and pressure ranges.

12. Figure S6. Average surface ozone concentrations from rural sites on the TOAR network over the whole world and biases between StratTrop and CRI-Strat model simulations and observations from TOAR network using data from 2010 to 2014, averaged over whole year (a-c), June to August (d-f) and December to February (g-i).

13. Figure S7. Average surface ozone concentrations from rural sites on the TOAR network over North America and biases between StratTrop and CRI-Strat model simulations and observations from TOAR network using data from 2010 to 2014, averaged over whole year (a-c), June to August (d-f) and December to February (g-i).

14. Figure S8. Average surface ozone concentrations from rural sites on the TOAR network over Europe and biases between StratTrop and CRI-Strat model simulations and observations from TOAR network using data from 2010 to 2014, averaged over whole year (a-c), June to August (d-f) and December to February (g-i). Mean bias between model and observations given in titles of panels b, c, e, f, h, and i.

15. Figure S9. Average surface ozone concentrations from rural sites on the TOAR network over East Asia and biases between StratTrop and CRI-Strat model simulations and observations from TOAR network using data from 2010 to 2014, averaged over whole year (a-c), June to August (d-f) and December to February (g-i). Mean bias between model and observations given in titles of panels b, c, e, f, h, and i.

16. Figure S10. Tropospheric ozone column (DU) in StratTrop mechanism in DJF (a) and JJA (b). Difference in tropospheric ozone column between CRI-Strat and StratTrop in DJF (c) and JJA (f). Difference in tropospheric ozone column between CRI_Emiss_ST and StratTrop in DJF(d) and JJA (g). Difference in tropospheric ozone column between CRI_Emiss_C2C3 and StratTrop in DJF(e) and JJA (h).

17. Figure S11. Difference in chemical production of Ox averaged over the lower 1km of the atmosphere between CRI-Strat and StratTrop (a), CRI_Emiss_ST and StratTrop (b), and CRI_Emiss_C2C3 and StratTrop (c). Difference in chemical loss of Ox averaged over lower 1 km of the atmosphere between CRI-Strat and StratTrop (d), CRI_Emiss_ST

and StratTrop (e), and CRI_Emiss_C2C3 and StratTrop (f). Difference in deposition of Ox averaged over lower 1 km of the atmosphere between CRI-Strat and StratTrop (g), CRI_Emiss_ST and StratTrop (h), and CRI_Emiss_C2C3 and StratTrop (i). Difference in deposition of Ox averaged over lower 1 km of the atmosphere between CRI-Strat and StratTrop (j), CRI_Emiss_ST and StratTrop (k), and CRI_Emiss_C2C3 and StratTrop (l).

18. Figure S12. Zonal mean flux though the $O(^1D) + H_2O$ reaction in StratTrop (a), and difference in zonal mean flux between CRI-Strat and StratTrop (b), CRI_Emiss_ST and StratTrop (c), and CRI_Emiss_C2C3 and StratTrop (d).

19. Figure S13. Mean differences in NO_x (a-c), NO_y (d-f), and NO_z (g-i) over the lower 1 km of the atmosphere between CRI-Strat and StratTrop (a, d, g), CRI_Emiss_ST and StratTrop (b, e and h), and CRI_Emiss_C2C3 and StratTrop (c, f, i).

20. Figure S14. Zonal mean flux through the OH + NO2 + M reaction in StratTrop (a), and difference in zonal mean flux between CRI-Strat and StratTrop (b), CRI_Emiss_ST and StratTrop (c), and CRI_Emiss_C2C3 and StratTrop (d).

21. Table S1. Structural codes and functional types used to describe CRI intermediates.

22. Table S2. Species treated by the CRI-Strat chemistry mechanism. Where the name of the species has been changed from that used by the original CRIv2-R5 mechanism in order to follow UKCA standards, the original name is also given. Species with 1 in the Strat column have been added to make the mechanism suitable for running in the stratosphere, species with 1 in the Aero column are only activated if running with GLOMAP-MODE.

23. Table S3. Photolysis reactions in the CRI-Strat chemical mechanism. Reactions with 1 in the Strat column have been added to make the mechanism suitable for running

in the stratosphere, reactions with 1 in the Aero column are only activated if running with GLOMAP-MODE. References for cross section data for reactions can be found in Telford et al. (2013). ?Reaction rates calculated online from the cross section data are multiplied by the scaling factor.

24. Table S4. Bimolecular reactions in CRI-Strat chemical mechanism. Reactions with 1 in the Strat column have been added to make the mechanism suitable for running in the stratosphere, reactions with 1 in the Aero column are only activated if running with GLOMAP-MODE. Temperature dependent reaction rate coefficients k_0, a_0 and b_0 are given for the equation $k(T) = k_0(T/300)^{a_0}\exp(-b_0/T)$, where T is temperature in K.

25. Table S5. Termolecular reactions in CRI-Strat chemical mechanism. Reactions with 1 in the Strat column have been added to make the mechanism suitable for running in the stratosphere, reactions with 1 in the Aero column are only activated if running with GLOMAP-MODE. Temperature and pressure dependent reaction rate coefficients k_1, a_1, b_1, k_2, a_2, b_2 and F are given for the equation $k(T) = (\frac{k_0(T)[M]}{1+k_0(T)[M]/k_i(T)})F_c^{(1+(log(k_0(T)/k_i))^2)^{-1}}$, where T is temperature in K; $[M]$ is the total number density in molecules cm^{-3}; $k_0 = k_1(T/300)^{a_1}\exp(-b_1/T)$ is the low pressure limit rate coefficient and $k_i = k_2(T/300)^{a_2}\exp(-b_2/T)$ is the infinite pressure limit rate coefficient. If $k_2 = 0$ then $k(T) = k_0(T)[M]$; if $k_1 = 0$ then $k(T) = k_i(T)$. The broadening term F_c is calculated from F as follows: if $0 > F < 1$ then $F_c = F$; if $F > 1$ then $F_c = \exp(-F/T)$; if $F = 0$ then the F_c term in the equation is ignored.

26. Table S6. Overview of tropospheric Ox burden, lifetime, ozone production efficiency (OPE), chemical production, chemical loss, deposition and inferred stratosphere to troposphere transfer. Values in brackets give fraction of total chemical production for

the production terms and fraction of total losses ($L_{Ox} + D_{Ox}$) for the loss and deposition terms.

27. Table S7. Overview of air mass weighted OH concentration, CO burden and CO lifetime.

28. Table S8. Overview of tropospheric oxidised nitrogen burdens (fraction of total NO_y in brackets), tropospheric oxidised nitrogen emission and deposition fluxes, stratosphere-troposphere transfer (STT) and NO_y lifetime in the troposphere (fraction of total NO_y deposition in brackets).

Additional Supporting Information (Files uploaded separately)

1. Table S2. CRI-Strat_species.xcls

2. Table S3. CRI-Strat_photol.xcls

3. Table S4. CRI-Strat_bimol.xcls

4. Table S5. CRI-Strat_termol.xcls

Introduction

This supplement provides additional data, results and analysis to support the main paper. It starts in Section S1 with a comparison of computational costs for the CRI-Strat and StratTrop mechanisms in UKCA run on the same model architecture. In then documents details of the CRI-Strat mechanism in Section S2. Here, we provide supporting tables in excel files which contain the entire CRI-Strat mechanism as used in UKCA. These tables were generated directly from the source code used by the model. Section S3 shows a comparison between the standard version of StratTrop and the version used in the paper, which contains some minor changes to make it conserve nitrogen to enable a fair comparison with CRi-Strat. Section S4 documents some differences in reaction rate

coefficients between the CRI-Strat and StratTrop mechanisms. Finally, Sections S5 and

S6 provide some supporting analysis of ozone and nitrogen containing species respectively

to support the analysis conducted in the main paper.

S1. Comparison of mechanism runtime

Both the CRI-Strat and StratTrop mechanisms were run in the UKCA model version 10.9 at $1.25° × 1.875°$ (N96) resolution with 85 vertical levels up to 85 km, as described in the main paper. Simulations were run on the the joint Met Office - NERC MONSooN2 supercomputer, which is a CRAY XC40 machine using Xeon E5-2695v4 18C 2.1GHz processors. The model simulations were carried out on 12 nodes with 36 cores per node for a total of 432 cores. Over the course of a year, the CRI-Strat run had an average runtime per month of $9056 ± 245$s, compared with $5170 ± 137$s for the StratTrop simulation. Hence the CRI-Strat simulation took 75.2% longer than StratTrop. Memory usage was 252Gb for CRI-Strat compared to 183Gb for StratTrop, an increase of 30%.

## S2. Details of the CRI-Strat mechanism

Each intermediate species in CRI is named using a code signifying its general structure, CRI index and functional group. For example, "RN10O2" is an n-aklyl peroxy radical with 10 $C − H$ and $C − C$ bonds (equivalent to the n-propyl peroxy radical, or "NC3H7O2" in the MCM). The radicals generated after the first few steps of oxidation will typically form intermediate lumped carbonyl species (labelled with "CARB") which can undergo further oxidation or photolysis. For example "CARB3" is a dicarbonyl with 3 C-H or C-C bonds (equivalent to glyoxal or "GLYOX" in MCM). An intermediate with a CRI index 3 higher than another intermediate is usually a related molecule with an alkyl chain one C-atom longer ($+1$ $C − C$ bond, $+2$ $C − H$ bonds). So "CARB6" is equivalent to methylglyoxal, called "MGLYOX" in MCM. Note that while smaller intermediates (CRI index $≤ 10$) generally have a single clear analogue species or represent a small group of isomers, larger intermediates often represent many different molecules which may have different chemical

November 23, 2020, 4:28pm

formulae and molecular masses. A full list of potential structure and functional codes are provided in Table S1.

Full documentation of all species and reactions in the CRI-Strat mechanism are given in Tables S2-S5. In many case species are renamed from how they appear in the original CRI mechanism, for example "CH3" is changed to "Me" and "C2H5" is changed to "Et". This is done both for consistency with how other species are named within UKCA and because there is a hard limit of 10 characters for each species name in ASAD. Those species and reactions with a number 1 in the Strat column are copied from the StratTrop mechanism, to add stratospheric chemistry to the base CRIv2-R5 scheme.

S3. Changes to StratTrop mechanism to conserve Nitrogen

In making the comparison of nitrogen reservoir species (NO_y) between CRI-Strat and StratTrop, it became clear that there was substantially less NO_y in StratTrop than there should be and there was no way of explain where it was going via the diagnostics used to carry out the NO_y budget analysis (see Fig. 13 and Table 9 in main paper). The cause of this problem was found to be these two reactions in StratTrop did not conserve NO_y:

$$DMS + NO_3 \rightarrow SO_2 \tag{1}$$

$$MONOTERP + NO_3 \rightarrow 0.26 * SEC\_ORG \tag{2}$$
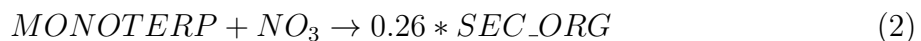
Both of these reactions are linked to the GLOMAP-mode aerosol scheme, and were copied from the offline oxidants version of the model (Mulcahy et al., 2020) in which concentrations of oxidants are prescribed and therefore unaffected by chemistry. However, when being used in a coupled model setup (such as in UKCA with the StratTrop mechanism), this means that the nitrogen in NO_3 is not being conserved, which would have knock on effects to the NO_y and Ox budgets. These reactions are simulated differently in CRI-Strat

due to its different handling of monoterpene and DMS chemistry, meaning that in CRI-Strat the nitrogen is conserved and tracked through diagnostics. Some minor changes were therefore made to the StratTrop scheme in order to enable a fair and rigorous comparison between the CRI-Strat and StratTrop mechanisms.

It was decided that the simplest solution to this problem would be for both of these reactions to make $HONO_2$ by replacing the two reactions with the following:

$$DMS + NO_3 \rightarrow SO_2 + HONO_2 \tag{3}$$

$$MONOTERP + NO_3 \rightarrow 0.26 * SEC\_ORG + HONO_2 \tag{4}$$

The $HONO_2$ produced is most likely to be lost via wet or dry deposition and have little further effect on chemistry (unless it is photolyzed or oxidised). However, it would be tracked by the diagnostics for NO_y deposition, enabling full conservation of reactive nitrogen. For the case of DMS, $HONO_2$ is a product of $NO_3 + DMS$ oxidation, as it proceeds via hydrogen abstraction (von Glasow & Crutzen, 2004), so this change to the reaction is reasonable. However, monoterpene oxidation via NO_3 typically proceeds with the NO_3 attaching to the double bond to form an organonitrate. In CRI-Strat, when NO_3 reacts with APINENE or BPINENE, the products will propagate, but the nitrogen is always conserved and its deposition is tracked via diagnostics, mostly likely as $RONO_2$ or as $HONO_2$ if when formed following further reaction. The monoterpene parameterisations are simplified in StratTrop, hence assuming $HONO_2$ is formed will enable tracking of NO_y that is in keeping with the rest of the mechanism, enabling a fair comparison with CRI-Strat.

In this section, we document differences between the original StratTrop mechanism (StratTrop_orig) with the modified version that conserves nitrogen (StratTrop_Ncon). In

November 23, 2020, 4:28pm

the main paper, the StratTrop_Ncon mechanism is used for all analysis and is simply referred to as StratTrop. Differences in zonal mean concentrations of $HONO_2$, NO_y, NO_x, NO_z and O_3 are shown in Figure S1. There is a considerable increase $HONO_2$, all of which is lost via reactions 1 and 2 in StratTrop_orig. There is a corresponding increase in NO_y and NO_z in StratTrop_Ncon due to the additional $HONO_2$. However, there is only slight increase in NO_x and O_3, showing that the additional $HONO_2$ in StratTrop_Ncon is mostly lost to deposition without having a huge influence on the overall composition of the atmosphere.

The differences between StratTrop_orig and StratTrop_Ncon are detailed further in the following tables. The conservation of nitrogen leads to an increase in tropospheric ozone burden of approximately 0.5%, as shown in Table S6. Production and loss terms for O_3 are similar but slightly higher in StratTrop_Ncon. Loss via NO_y deposition is also higher, although this is an artifact because StratTrop_orig does not have a full diagnostic of O_x loss because it is missing the fluxes via reactions 1 and 2. Due to how the stratosphere-troposphere transport (STT) of ozone is calculated from the difference in production and loss of O_x, StratTrop_orig also underestimates how much tropospheric ozone is coming from the stratosphere.

Table S7 shows that OH is slightly higher in StratTrop_Ncon, presumably from $HONO_2$. However, this has only a small impact on CO burden and lifetime.

Table S8 documents the changes to the NO_y in StratTrop_Ncon compared to Strat-Trop_orig. The $HONO_2$ burden is 4.5% larger in StratTrop_Ncon compared to Strat-Trop_orig, however this leads to a 7.9% increase in total NO_y due to the large contribution of deposition via $HONO_2$. In StratTrop_orig, this large fraction of NO_y loss is missing

from the diagnostics, which leads to invalid results where the calculated total emissions are greater than total deposition, implying that net flux of NO_y is into the stratosphere rather than from the stratosphere.

S4. Differences in reaction rates coefficients between mechanisms

The version of the CRI mechanism used for these developments was CRIv2-R5, as documented by M. Jenkin, Watson, Utembe, and Shallcross (2008); Watson, Shallcross, Utembe, and Jenkin (2008); S. R. Utembe, Watson, Shallcross, and Jenkin (2009); the same version used in the WRF-Chem model (Archer-Nicholls et al., 2014) and STOCHEM-CRI model (S. Utembe et al., 2010; Khan et al., 2015). CRIv2-R5 was merged with the stratospheric component of the StratTrop mechanism to make the whole-atmosphere version of the mechanism evaluated in this paper.

Chemical mechanism developers often make use of the most up-to-date kinetic information as possible. However, as improvements are made in experimental techniques and *ab initio* methods, kinetic information (rate constants, product yields etc) change with time. This can be seen through the updates in the evaluations of kinetic data for use in atmospheric chemistry modelling (Sander et al., 2011; Atkinson, 2000). The CRIv2-R5 mechanism was originally optimised against the MCMv3.1 (M. E. Jenkin et al., 2003; Saunders et al., 2003), which drew heavily on kinetic parameters evaluated by the IUPAC Task Group on Atmospheric Chemical Kinetic Data Evaluation (e.g., Atkinson et al. (1997, 2004)). The StratTrop scheme (Archibald et al., 2020) drew on a mixture of data from the MCMv3.2 website, the IUPAC Task Group web pages and the NASA JPL Evaluation No. 17 (Sander et al., 2011).

In this section, differences in reaction rate coefficients for key bimolecular and termolecular reactions are documented and commented on where relevant. There are some reactions which are out of date in CRI-Strat, and in more up-to-date versions (e.g. version 2.2 M. E. Jenkin et al. (2019)) the updated reaction rate coefficients is either identical or closer

to StratTrop. In other cases, the reactions are simply different, with CRI-Strat drawing from IUPAC evaluations and StratTrop from JPL. In these cases, it is not straightforward to say which mechanism is right. These cumulative differences in reaction rate coefficients are a driving factor in why the CRI_Emiss_ST scenario, in which the CRI-Strat mechanism is run with StratTrop emissions, differs from the StratTrop run.

We first document differences in termolecular reactions in Figure S5. CRI-Strat forms $HONO_2$ faster under all atmospheric conditions, particularly in colder low pressure conditions present in the upper atmosphere. HONO is also formed more rapidly. In both cases, these increase the rate of transfer from reactive NO_x into reservoir species. HO_2NO_2 is formed faster in the lower atmosphere in CRI-Strat, and PAN is also formed faster under most atmospheric conditions, but both of these important reservoir species are more thermally unstable in CRI-Strat, resulting in more HO_2NO_2 and PAN near emission sources but less in the free troposphere. Formation of MPAN is approximately 50 times faster in StratTrop than in CRI-Strat, one of the largest differences in reaction rates between the mechanisms. This causes substantial changes to chemistry in regions dominated by BVOC emissions, as MACRO2 (or RU10O2 in CRI-Strat) is formed in the degradation of isoprene.

The set of $O(^1D)$ reactions with H_2O, N_2 and O_2 are extremely important for tropospheric chemistry as the $O(^1D) + H_2O$ reaction is both the major source of the OH radical and a key sink of O_x, whereas the $O(^1D) + N_2$ and $O(^1D) + O_2$ (collectively $O(^1D) + M$) reactions stabilise the exited odd oxygen into its ground electronic state. In CRIv2, the $O(^1D) + H_2O$ reaction rate coefficient is faster and the $O(^1D) + N_2$ coefficient slower compared to StratTrop. Collectively, these differences mean any $O(^1D)$ atom is between 20 to

25% more likely to react with H_2O in CRI-Strat than in StratTrop, as shown in Figure S2, leading to shorter O_x lifetime and higher HO_x production in CRI-strat, leading to net loss of ozone in Southern hemisphere in CRI-Strat, and loss of ozone across the troposphere in CRI_Emiss_ST and CRI_Emiss_C2C3, compared to StratTrop as shown in Figure S10.

Figure S3 compares reaction rates of all inorganic bimolecular reactions that differ between CRI-Strat and StratTrop, except for the $O(^1D)$ reactions documented in Figure S2. All other inorganic bimolecular reactions are identical in both mechanisms. The $O_x + NO_x$ reactions are subtly different between the mechanisms; it is hard to say how significant these changes would be but the faster $O_3 + NO$ reaction in CRI-Strat at boundary layer temperatures would lead to faster titration of ozone in polluted regions. $HO_2 + NO$ is approximately 9% faster in CRI-Strat across all temperatures, leading to faster O_x production The $OH + HO_2NO_2$ reactions faster in CRI-Strat, lowering the lifetime of this key reservoir species. $OH + H_2$ is slightly slower in CRI-Strat. The $HO_2 + HO_2$ reaction is faster in CRI-Strat, leading to a greater HO_x sink.

Figure S4 compares reaction rates of selected organic bimolecular reactions that differ between CRI-Strat and StratTrop. Due to there being many more organic reaction, this section focuses on those which have a large flux in the troposphere so are important for ozone formation, and for which both mechanisms share the same or similar reactions. The $OH + CH_4$ is slightly faster in CRI-Strat compared to StratTrop, this is not a big difference but it in an important reaction for atmospheric composition and does affect calculations of methane lifetime (Table 6 in main paper). $MeO_2 + NO$ is faster in StratTrop, could aid Ox production away from emission sources in StratTrop and more rapid production of $MeONO_2$. The $OH + MeONO_2$ is 20-100 times faster over typical temperature range in

CRI-Strat compared to StratTrop, and has the opposite temperature dependence, results in much less $MeONO_2$ in CRI-Strat and loss of an important reservoir species. This is one of the largest differences in reaction rate coefficients between the mechanisms. OH+PAN faster in CRI-Strat, contributing to PAN having a shorter lifetime in CRI-Strat. $OH + C_5H_8$ and $OH + MeCHO$ are slightly faster in CRI-Strat, whereas $OH + EtCHO$ is faster in StratTrop.

Collectively, all these differences help explain why CRI_Emiss_ST has less NO_x than StratTrop, as the NO_x is more rapidly taken up into reservoir species that can are deposited out. The only exception being the formation of MPAN, which occurs in much greater burdens in StratTrop than CRI-Strat.

S5. Supporting Analysis of ozone

To support Figure 1 in the main paper, Figures S7, S8 and S9 show comparisons between the CRI-Strat and StratTrop model simulations and the TOAR network with a focus on North America, European and East Asian regions respectively, with the majority of the East Asian region site located in Japan. In all three cases, both mechanisms have a low bias compared to observations in winter and a high bias in summer, but CRI-Strat has higher surface ozone throughout the year. Both mechanisms also tend to have a higher bias over low latitude regions and a lower bias over high latitude regions. In North America and Europe, StratTrop is overall biased low over the whole year (-2.2 ppbv and -2.3 ppbv respectively) while CRI-Strat has a high bias (+2.8 ppbv and +2.1 ppbv; Figures S7 and S8). In contrast, StratTrop has a small high bias over the East Asian region (2.8 ppbv) while CRI-Strat has a much higher bias (12.7 ppbv; Figure S9).

Tropospheric ozone in the StratTrop scenario and in comparison to all of the other model scenarios are shown in Figure S10. Tropospheric ozone is higher in the polluted northern hemisphere and lower in the cleaner southern hemisphere in the CRI-Strat simulation compared to StratTrop. CRI_Emiss_ST and CRI_Emiss_C2C3 both have much lower ozone compared to StratTrop across the world. These results indicate that the increased northern hemisphere ozone in CRI-Strat is due to the increase in anthropogenic NMVOC emissions, while the decreased ozone in the southern hemisphere is largely due to different kinetic parameters in CRI-Strat, as explained in Section 1.

Figure S11 shows differences in production and loss of odd oxygen (Ox) in the lowest 1km of the atmosphere between the model scenarios. Production and loss of Ox is typically higher in all scenarios that use the CRI-Strat mechanism compared to Strattrop, but

November 23, 2020, 4:28pm

this is most apparent in the base CRI-Strat scenario. The CRI_Emiss_C2C3 scenario is similar to CRI_Emiss_ST, but has slightly faster production in polluted regions such as the Indo-Gangentic plain.

The difference in flux through the $O(^1D) + H_2O$ drives much of the difference in loss of Ox between the CRI-Strat mechanism and StratTrop, as can be seen if you compare Figure S12 with Figure 8 (d-f) in the main paper. The reaction rate coefficients for the $O(^1D)$ reactions in StratTrop and CRI-Strat are compared in Section 1.

S6. Supporting Analysis of Nitrogen Containing Species

Differences in NO_x, NO_y and NO_z summed species for the lowest 1 km of the atmosphere are shown in Figure S13. There is a clear trend for reduced NO_x and higher NO_z in the CRI-Strat mechanism compared to StratTrop (Fig. S13 (a, c)), with more NO_y everywhere except the highly polluted East Asia and India regions. The CRI-STEmiss and CRI_Emiss_C2C3 simulations have lower NO_x and NO_y almost everywhere compared to StratTrop (Fig. S13 (b, c, e, f)), and the only regions with higher NO_z are downwind of pollution centres such as East Asia, Western Europe and the Indo Gangentic plain (Fig. S13 (h, i)). Overall, CRI-Strat forms HONO2 faster than StratTrop in polluted regions (see Section 1), causing net loss of NO_y in CRI-STEmiss and CRI_Emiss_C2C3. However, with the extra NMVOC emissions in CRI-Strat, more of the NO_y is locked up as $RONO_2$ which generally have longer lifetimes than $HONO_2$ and so CRI-Strat has more NO_y everywhere except in very polluted regions where $HONO_2$ production dominates.

Differences in flux through the $OH + NO_2 + M$ reaction are shown in Figure S14. CRI-Strat has much greater flux through this reaction near the surface, due to the higher concentrations of HO_x in the CRI-Strat simulation. However, away from emission sources, the flux becomes lower in CRI-Strat due to it having NO_x concentrations compared to StratTrop as more of the NO_x is converted into reservoir species. The CRI_Emiss_ST simulation has somewhat greater flux through $OH + NO_2 + M$ than StratTrop through the boundary layer. These differences are mostly driven by the differences in OH and NO2 between the schemes, as although the reaction rate coefficient for the $OH + NO_2 + M$ reaction differs between the mechanisms, it is a relatively small change over the temperature and pressure range of the boundary layer (see Section 1).

November 23, 2020, 4:28pm

References

Archer-Nicholls, S., Lowe, D., Utembe, S., Allan, J., Zaveri, R. A., Fast, J. D., . . . McFiggans, G. (2014, nov). Gaseous chemistry and aerosol mechanism developments for version 3.5.1 of the online regional model, WRF-Chem. *Geoscientific Model Development*, *7*, 2557–2579. Retrieved from `http://www.geosci-model-dev.net/7/2557/2014/` doi: 10.5194/gmd-7-2557-2014

Archibald, A., O'Connor, F., Abraham, N. L., Archer-Nicholls, S., Chipperfield, M., Dalvi, M., . . . Zeng, G. (2020). Description and evaluation of the UKCA stratosphere-troposphere chemistry scheme (StratTrop vn 1.0) implemented in UKESM1. *Geoscientific Model Development*, *13*, 1223–1266. doi: 10.5194/gmd-2019-246

Atkinson, R. (2000). Atmospheric chemistry of VOCs and NOx. *Atmospheric Environment*, *34*, 2063–2101. Retrieved from `http://linkinghub.elsevier.com/retrieve/pii/S1352231099004604` doi: 10.1016/S1352-2310(99)00460-4

Atkinson, R., Baulch, D. L., Cox, R. A., Crowley, J. N., Hampson, R. F., Hynes, R. G., . . . Rossi, M. J. (2004). Evaluated kinetic and photochemical data for atmospheric chemistry : Volume I – gas phase reactions of Ox, HOx, NOx and SOx species. *Atmospheric Chemistry and Physics*, *4*, 1461–1738.

Atkinson, R., Baulch, D. L., Cox, R. A., Hampson, R. F., Kerr, J. A., Rossi, M. J., & Troe, J. (1997). Evaluated Kinetic and Photochemical Data for Atmospheric Chemistry Supplement VI. *J. Phys. chem. Ref. Data*, *26*(6), 1329–1499.

Jenkin, M., Watson, L., Utembe, S., & Shallcross, D. (2008, oct). A Common Representative Intermediates (CRI) mechanism for VOC degradation. Part 1: Gas phase mechanism development. *Atmospheric Environment*, *42*, 7185–7195. Retrieved

from `http://linkinghub.elsevier.com/retrieve/pii/S1352231008006742` doi: 10.1016/j.atmosenv.2008.07.028

Jenkin, M. E., Khan, M. A., Shallcross, D. E., Bergström, R., Simpson, D., Murphy, K. L., & Rickard, A. R. (2019). The CRI v2.2 reduced degradation scheme for isoprene. *Atmospheric Environment*, *212*(May), 172–182. doi: 10.1016/j.atmosenv .2019.05.055

Jenkin, M. E., Saunders, S. M., Wagner, V., & Pilling, M. J. (2003, feb). Protocol for the development of the Master Chemical Mechanism, MCM v3 (Part B): tropospheric degradation of aromatic volatile organic compounds. *Atmospheric Chemistry and Physics*, *3*(1), 181–193. Retrieved from `http://www.atmos-chem-phys.net/3/181/ 2003/` doi: 10.5194/acp-3-181-2003

Khan, M. A. H., Cooke, M. C., Utembe, S. R., Archibald, A. T., Derwent, R. G., Xiao, P., . . . Shallcross, D. E. (2015). Global modeling of the nitrate radical (NO3) for present and pre-industrial scenarios. *Atmospheric Research*, *164-165*(3), 347–357. doi: 10.1016/j.atmosres.2015.06.006

Mulcahy, J. P., Johnson, C., Jones, C., Povey, A., Sellar, A., Scott, C. E., . . . Yool, A. (2020). Description and evaluation of aerosol in UKESM1 and HadGEM3-GC3.1 CMIP6 historical simulations. *Geoscientific Model Development*.

Sander, S. P., Friedl, R. R., Barker, J. R., Golden, D. M., Kurylo, M. J., Sciences, G. E., . . . Orkin, V. L. (2011). Chemical Kinetics and Photochemical Data for Use in Atmospheric Studies Evaluation Number 17 NASA Panel for Data Evaluation :. (17).

Saunders, S. M., Jenkin, M. E., Derwent, R. G., & Pilling, M. J. (2003, feb). Protocol for

the development of the Master Chemical Mechanism, MCM v3 (Part A): tropospheric degradation of non-aromatic volatile organic compounds. *Atmospheric Chemistry and Physics*, *3*, 161–180. doi: 10.5194/acp-3-161-2003

Telford, P. J., Abraham, N. L., Archibald, A. T., Braesicke, P., Dalvi, M., Morgenstern, O., ... Pyle, J. A. (2013). Implementation of the Fast-JX Photolysis scheme into the UKCA component of the MetUM chemistry climate model. *Geoscientific Model Development*, *6*, 161–177. doi: 10.5194/gmdd-5-3217-2012

Utembe, S., Cooke, M., Archibald, A. T., Jenkin, M., Derwent, R., & Shallcross, D. (2010, apr). Using a reduced Common Representative Intermediates (CRIv2-R5) mechanism to simulate tropospheric ozone in a 3-D Lagrangian chemistry transport model. *Atmospheric Environment*, *44*(13), 1609–1622. Retrieved from `http://linkinghub.elsevier.com/retrieve/pii/S1352231010001056` doi: 10 .1016/j.atmosenv.2010.01.044

Utembe, S. R., Watson, L. A., Shallcross, D. E., & Jenkin, M. E. (2009, apr). A Common Representative Intermediates (CRI) mechanism for VOC degradation. Part 3: Development of a secondary organic aerosol module. *Atmospheric Environment*, *43*(12), 1982–1990. Retrieved from `http://linkinghub.elsevier.com/retrieve/pii/S1352231009000284` doi: 10.1016/j.atmosenv.2009.01.008

von Glasow, R., & Crutzen, P. J. (2004, apr). Model study of multiphase DMS oxidation with a focus on halogens. *Atmospheric Chemistry and Physics*, *4*(3), 589–608. Retrieved from `http://www.atmos-chem-phys.net/4/589/2004/` doi: 10.5194/acp-4-589-2004

Watson, L., Shallcross, D., Utembe, S., & Jenkin, M. (2008, oct). A Common Repre-

sentative Intermediates (CRI) mechanism for VOC degradation. Part 2: Gas phase mechanism reduction. *Atmospheric Environment*, *42*(31), 7196–7204. Retrieved from http://linkinghub.elsevier.com/retrieve/pii/S1352231008006845 doi: 10.1016/j.atmosenv.2008.07.034
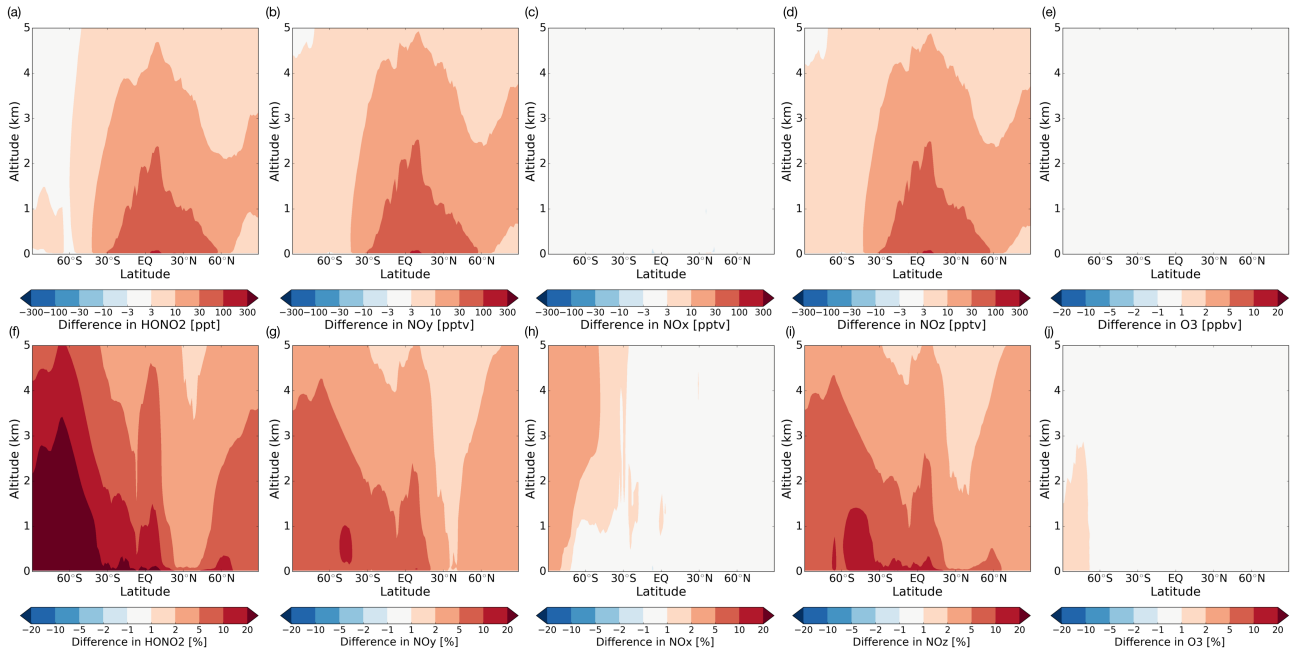
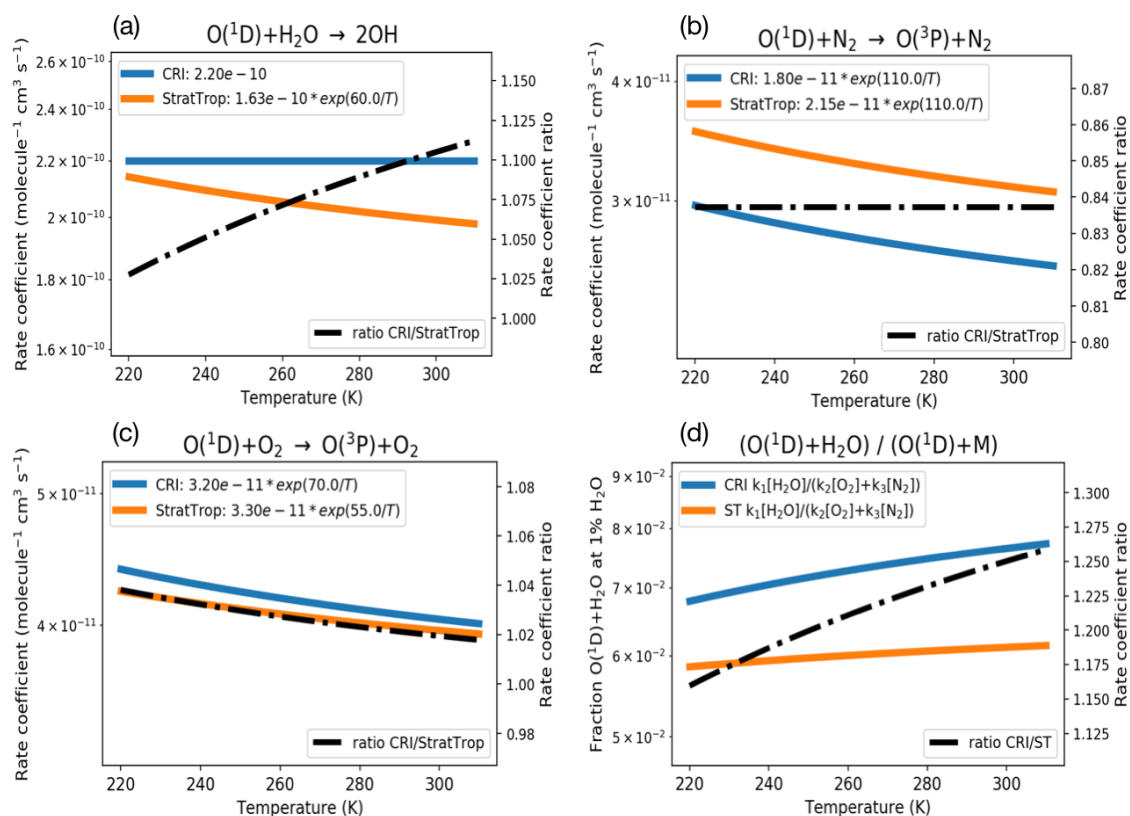**Figure S1.**   Difference in zonal mean $HONO_2$, NO_y, NO_x, NO_z and O_3 between Strat-Trop_NCon and StratTrop_Orig.

Figure S2. Comparison of selected inorganic bimolecular reaction rates in CRIv2 to equivalent reactions in StratTrop over an atmospherically relevant temperature range. Blue line is CRI rate, orange line StratTrop, both using scale on left axis, and black dot-dashed line shows ratio of CRI/StratTrop.
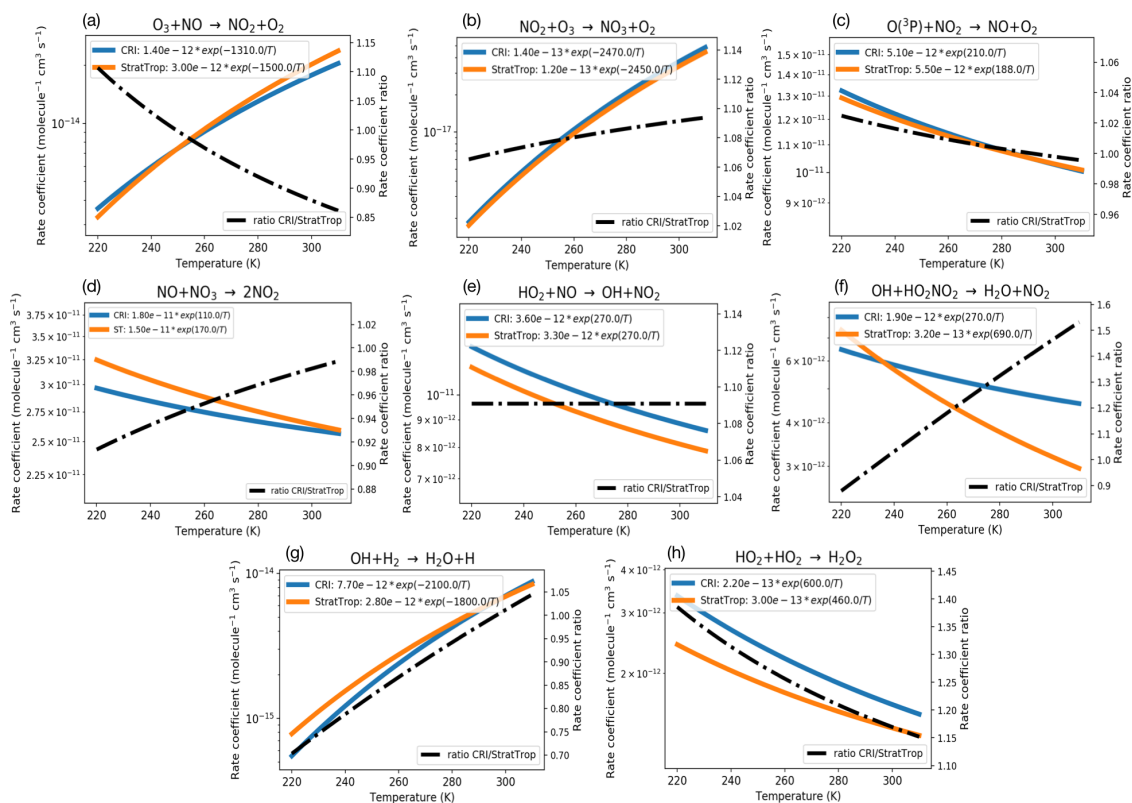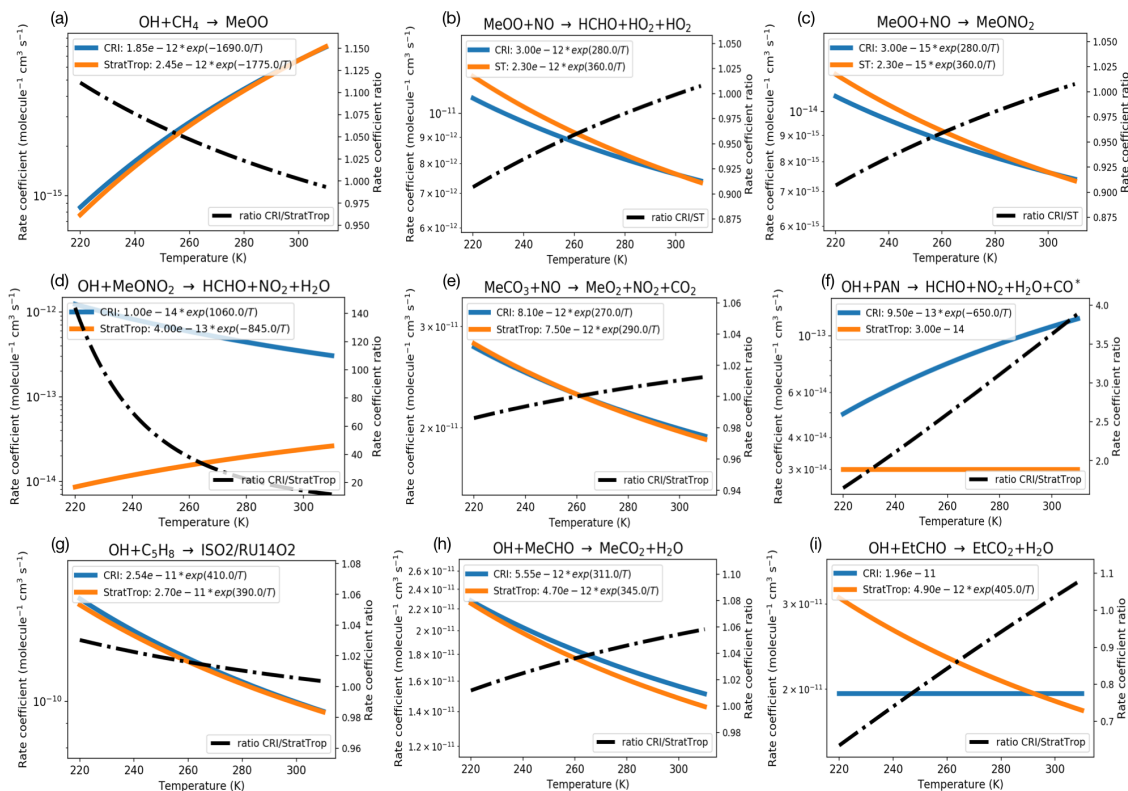
Figure S3. Comparison of inorganic bimolecular reaction rates in CRIv2 to equivalent reactions in StratTrop over an atmospherically relevant temperature range. Blue line is CRI rate, orange line StratTrop, both using scale on left axis, and black dot-dashed line shows ratio of CRI/StratTrop.
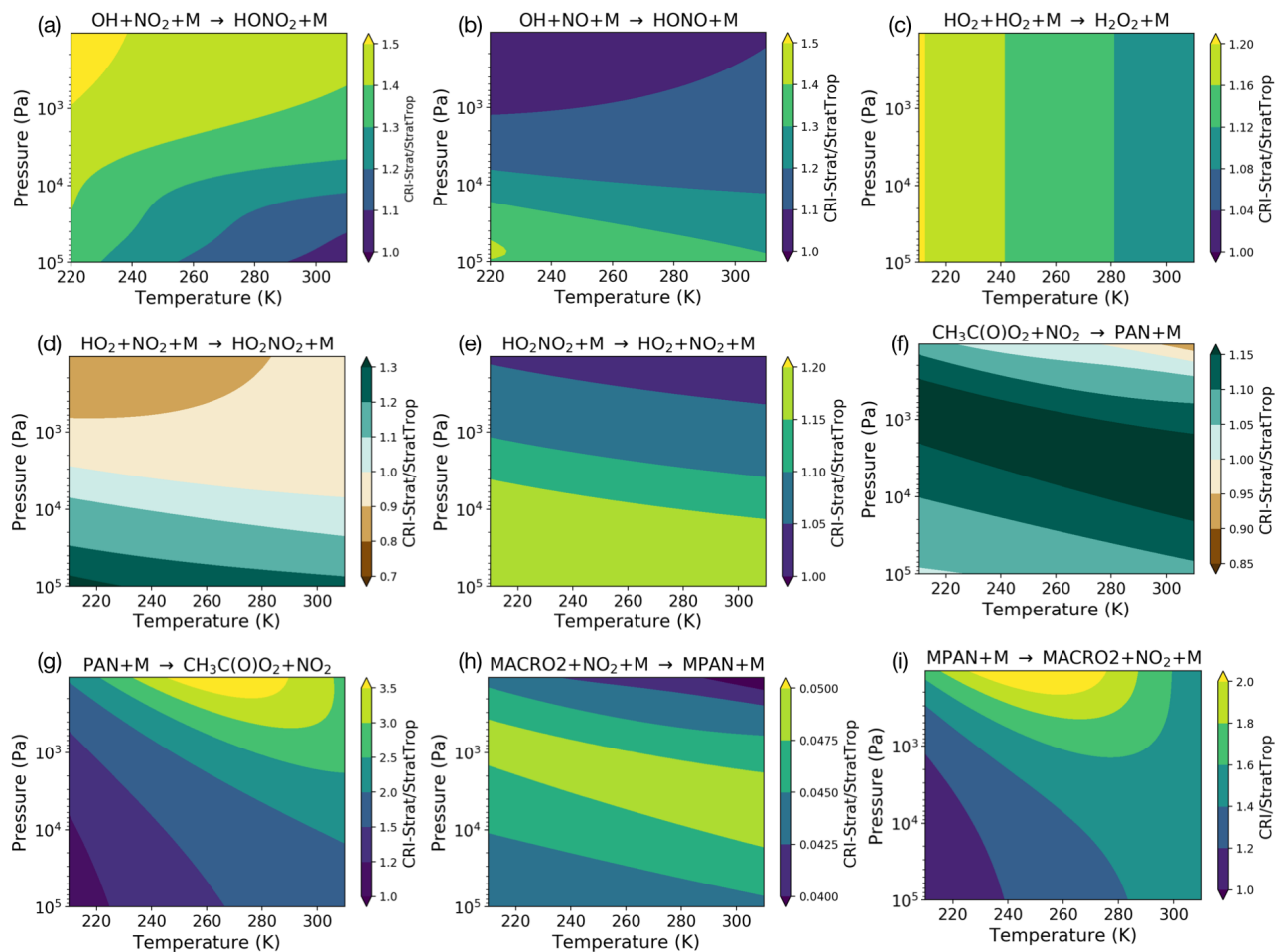
Figure S4. Comparison of selected organic bimolecular reaction rates in CRIv2 to equivalent reactions in StratTrop over an atmospherically relevant temperature range. Blue line is CRI rate, orange line StratTrop, both using scale on left axis, and black dot-dashed line shows ratio of CRI/StratTrop.

Figure S5.   Ratios of selected termolecular reaction rate coefficients in CRIv2 to equivalent reactions in StratTrop over atmospherically relevant temperature and pressure ranges.
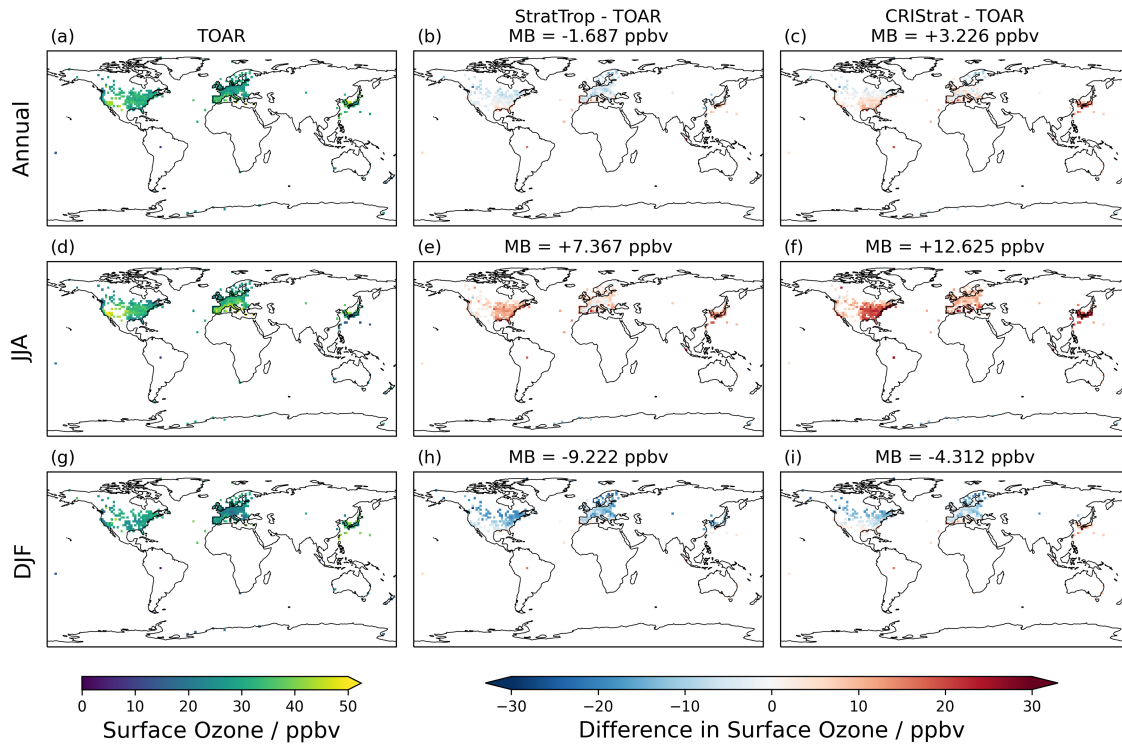
Figure S6. Average surface ozone concentrations from rural sites on the TOAR network across the world and biases between StratTrop and CRI-Strat model simulations and observations from TOAR network using data from 2010 to 2014, averaged over whole year (a-c), June to August (d-f) and December to February (g-i). Mean bias between model and observations given in titles of panels b, c, e, f, h, and i.
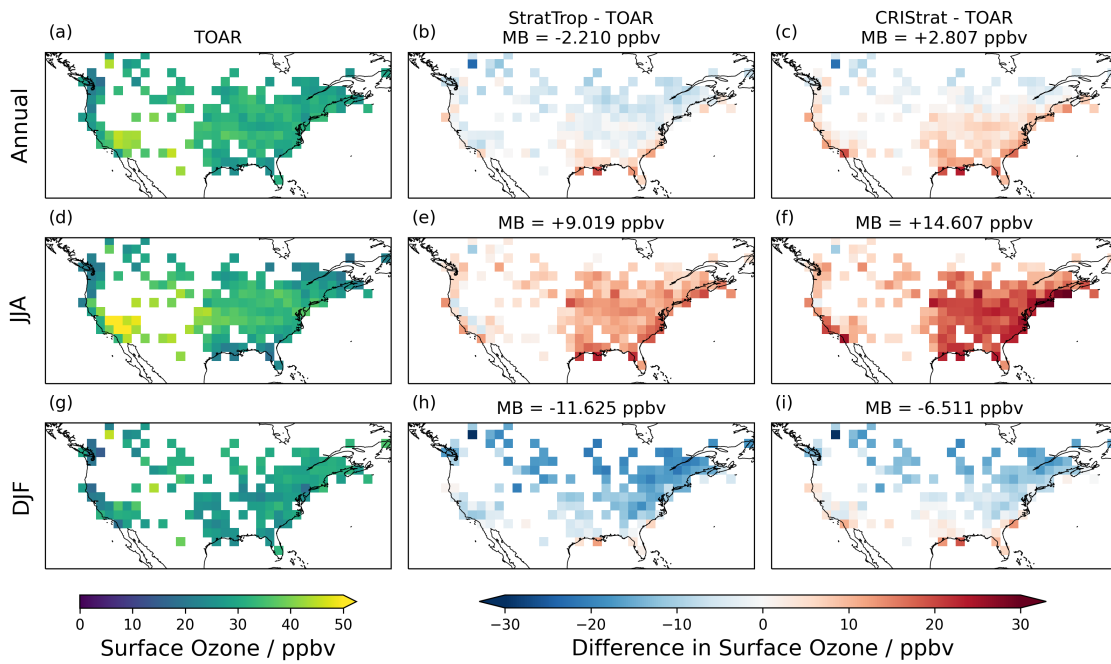
Figure S7. Average surface ozone concentrations from rural sites on the TOAR network over North America and biases between StratTrop and CRI-Strat model simulations and observations from TOAR network using data from 2010 to 2014, averaged over whole year (a-c), June to August (d-f) and December to February (g-i). Mean bias between model and observations given in titles of panels b, c, e, f, h, and i.

November 23, 2020, 4:28pm

Figure S8. Average surface ozone concentrations from rural sites on the TOAR network over Europe and biases between StratTrop and CRI-Strat model simulations and observations from TOAR network using data from 2010 to 2014, averaged over whole year (a-c), June to August (d-f) and December to February (g-i). Mean bias between model and observations given in titles of panels b, c, e, f, h, and i.
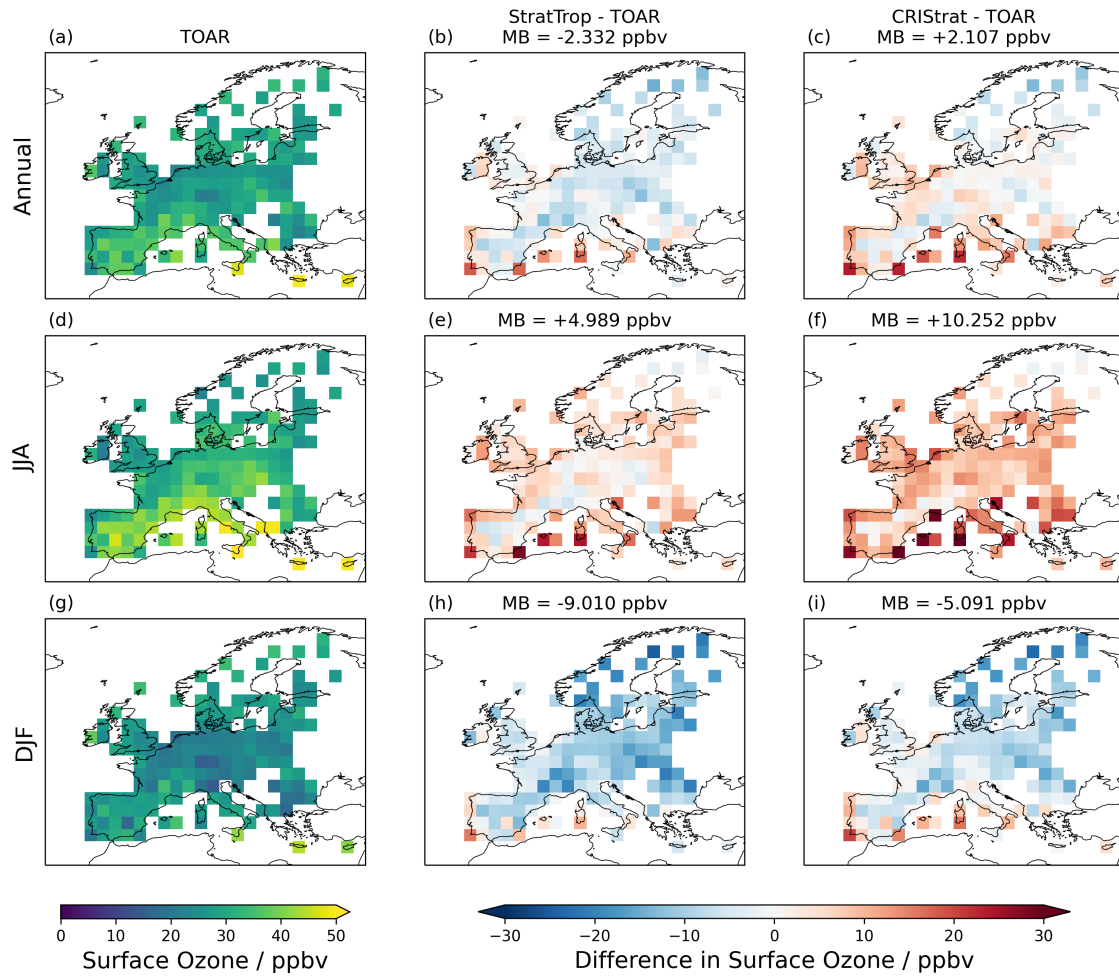
Figure S9. Average surface ozone concentrations from rural sites on the TOAR network over East Asia and biases between StratTrop and CRI-Strat model simulations and observations from TOAR network using data from 2010 to 2014, averaged over whole year (a-c), June to August (d-f) and December to February (g-i). Mean bias between model and observations given in titles of panels b, c, e, f, h, and i.
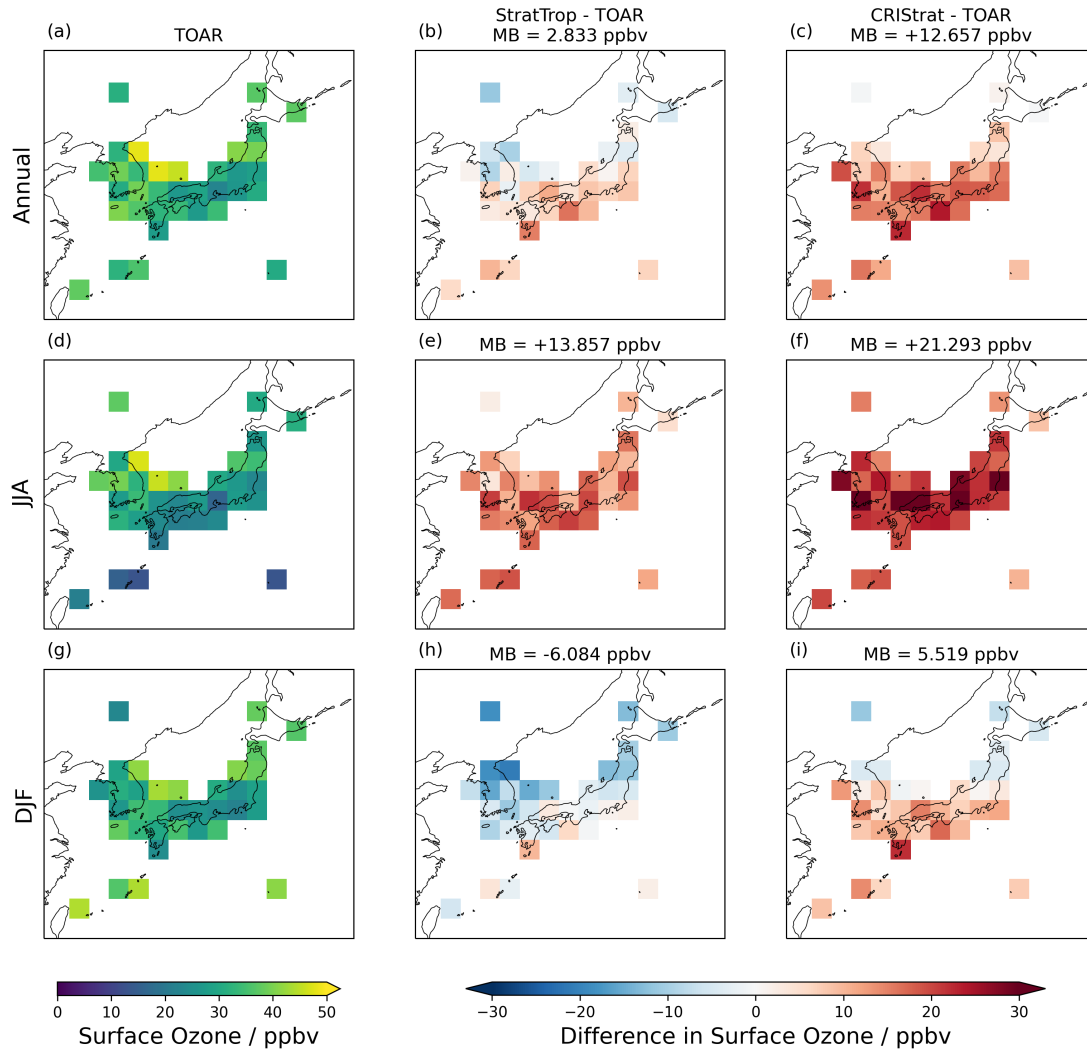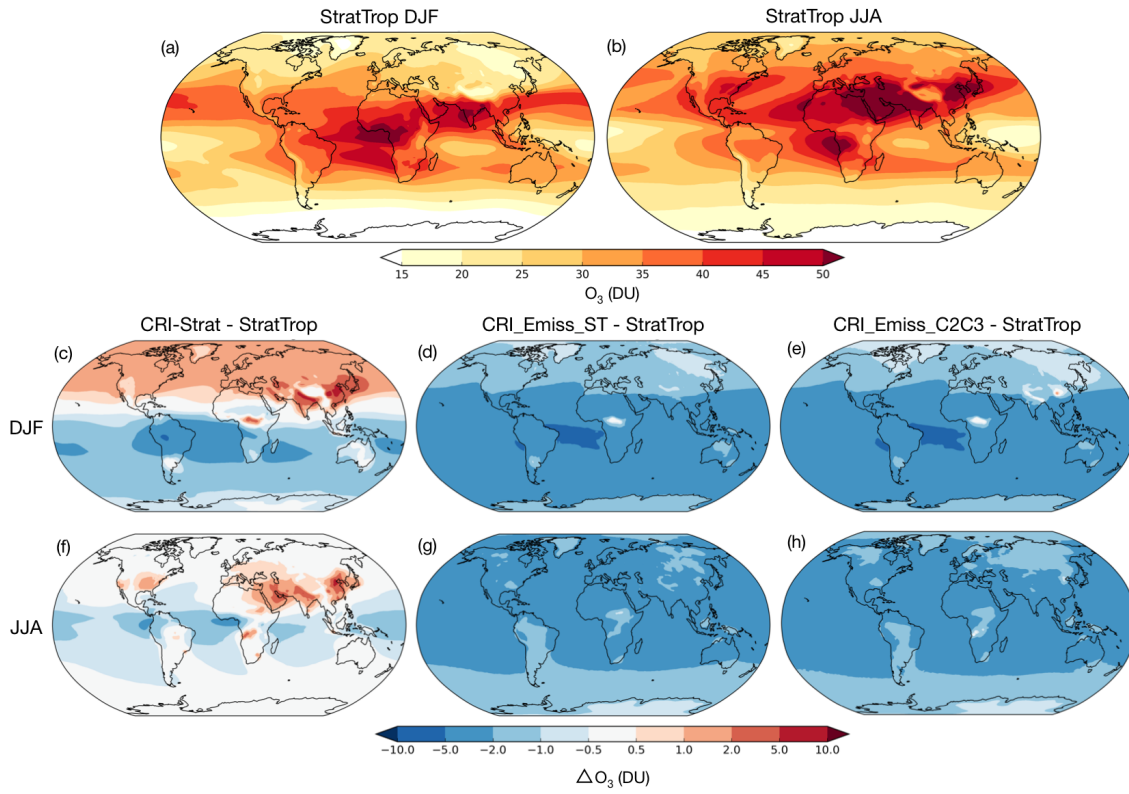
November 23, 2020, 4:28pm

Figure S10. Tropospheric ozone column (DU) in StratTrop mechanism in DJF (a) and JJA (b). Difference in tropospheric ozone column between CRI-Strat and StratTrop in DJF (c) and JJA (f). Difference in tropospheric ozone column between CRI_Emiss_ST and StratTrop in DJF(d) and JJA (g). Difference in tropospheric ozone column between CRI_Emiss_C2C3 and StratTrop in DJF(e) and JJA (h).
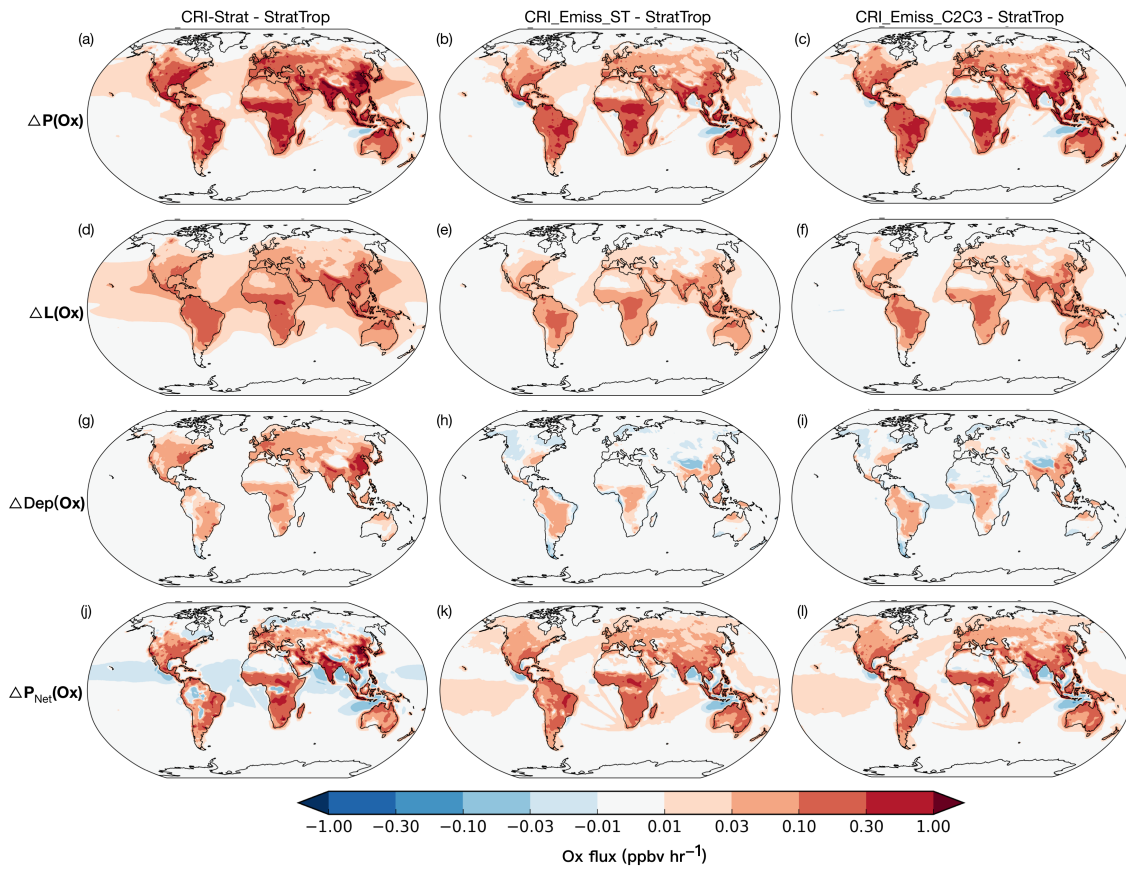
Figure S11. Difference in chemical production of Ox averaged over the lower 1km of the atmosphere between CRI-Strat and StratTrop (a), CRI_Emiss_ST and StratTrop (b), and CRI_Emiss_C2C3 and StratTrop (c). Difference in chemical loss of Ox averaged over lower 1 km of the atmosphere between CRI-Strat and StratTrop (d), CRI_Emiss_ST and StratTrop (e), and CRI_Emiss_C2C3 and StratTrop (f). Difference in deposition of Ox averaged over lower 1 km of the atmosphere between CRI-Strat and StratTrop (g), CRI_Emiss_ST and StratTrop (h), and CRI_Emiss_C2C3 and StratTrop (i). Difference in deposition of Ox averaged over lower 1 km of the atmosphere between CRI-Strat and StratTrop (j), CRI_Emiss_ST and StratTrop (k), and CRI_Emiss_C2C3 and StratTrop (l).

Figure S12. Zonal mean flux though the $O(^1D) + H_2O$ reaction in StratTrop (a), and difference in zonal mean flux between CRI-Strat and StratTrop (b), CRI_Emiss_ST and StratTrop (c), and CRI_Emiss_C2C3 and StratTrop (d).

November 23, 2020, 4:28pm

Figure S13.   Mean differences in NO_x (a-c), NO_y (d-f), and NO_z (g-i) over the lower 1 km of the atmosphere between CRI-Strat and StratTrop (a, d, g), CRI_Emiss_ST and StratTrop (b, e and h), and CRI_Emiss_C2C3 and StratTrop (c, f, i).
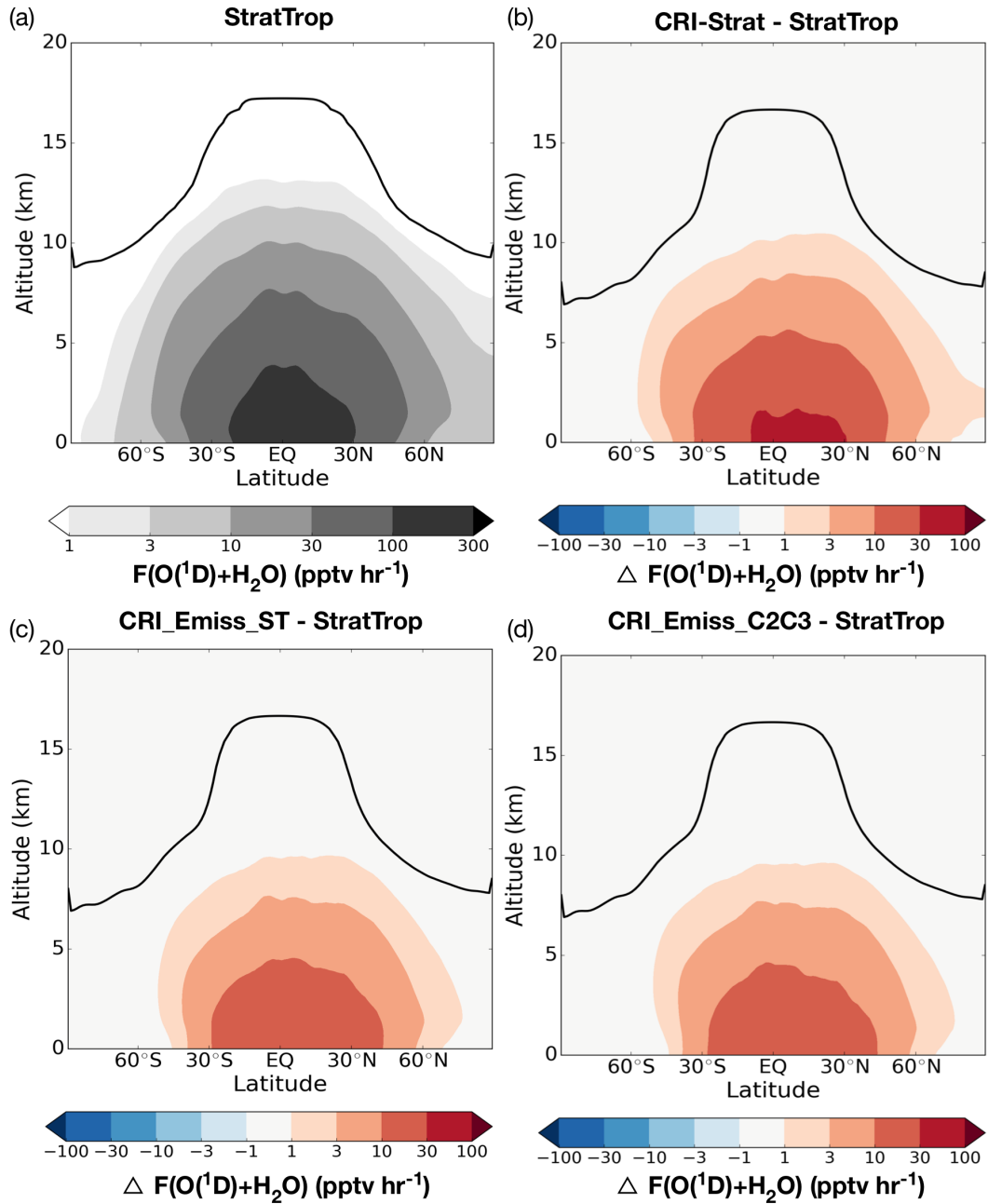
November 23, 2020, 4:28pm

Figure S14. Zonal mean flux through the $OH + NO2 + M$ reaction in StratTrop (a), and difference in zonal mean flux between CRI-Strat and StratTrop (b), CRI_Emiss_ST and StratTrop (c), and CRI_Emiss_C2C3 and StratTrop (d).
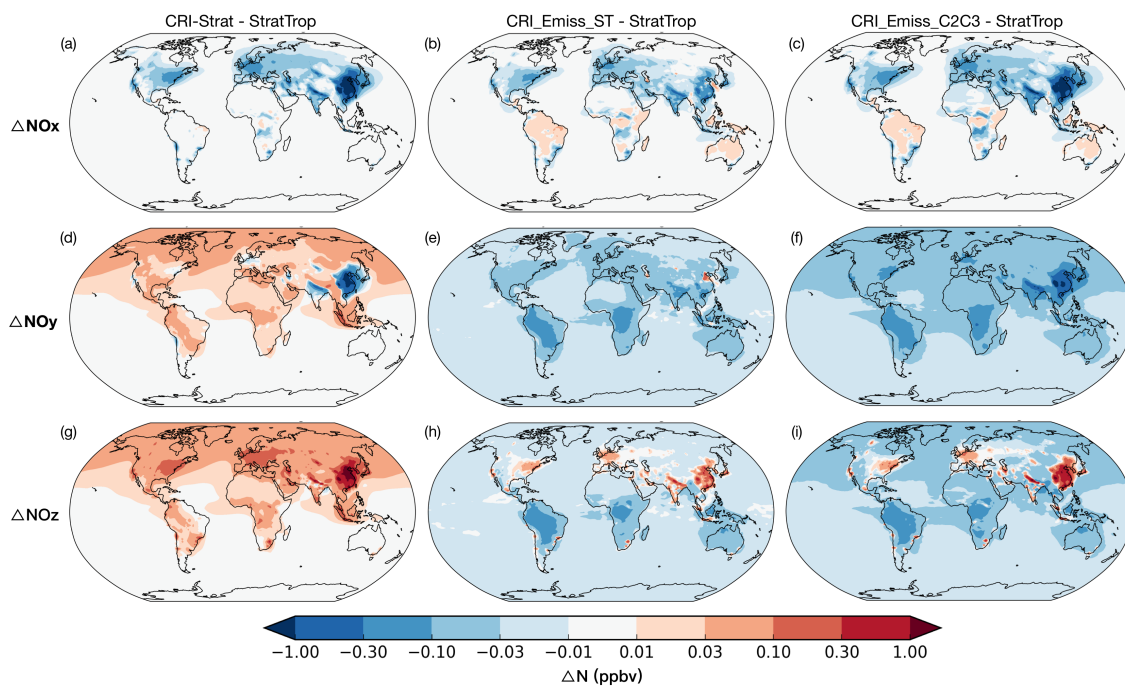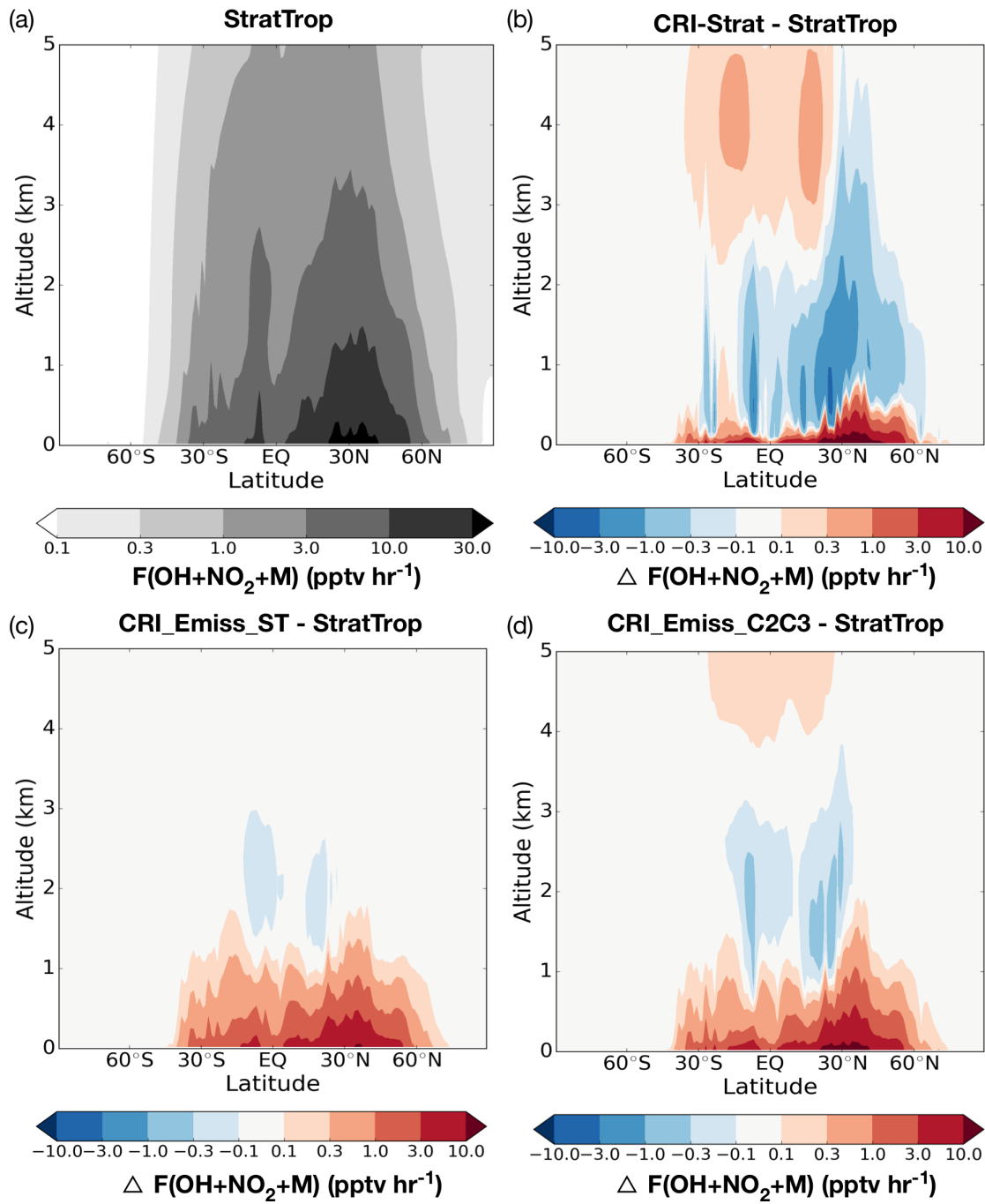
Table S1. Structural codes and functional types used to describe CRI intermediates.

Structural Code	Definition
RN-	Generic N-alkyl radical
NRN-	N-alkyl radical from NO3+alkene oxidation with nitrate group
RA-	Radical from aromatic oxidation
RU-	Unsaturated radical from C5H8 oxidation
NRU-	Unsaturated radical from NO3+C5H8 oxidation with nitrate group
RTN-	Radical from APINENE oxidation
NRTN-	Radical from NO3+APINENE oxidation with nitrate group
RTX-	Radical from BPINENE oxidation
NRTX-	Radical from NO3+BPINENE oxidation with nitrate group
RCOOH-	Carboxylic acid
CARB-	Generic carbonyl
UDCARB-	Second generation dicarbonyl from aromatic oxidation
UCARB-	Unsaturated carbonyl from C5H8 oxidation
NUCARB-	Second generation carbonyl product of Isoprene+NO3 oxidation with nitrate
TNCARB-	Second generation carbonyl product of APINENE oxidation
CCARB-	Second generation carbonyl product of BPINENE oxidation
TXCARB-	Second generation carbonyl product of BPINENE+O3 oxidation
AROH-	Phenol
RAROH-	Phenol radical
ARNOH-	Nitrophenol
Functional Group Code	Definition
-O2	Peroxy radical
-OOH	Peroxide
-NO3	Nitrate
-PAN	Peroxyacyl nitrate

Table S2. Species treated by the CRI-Strat chemistry mechanism. Where the name of the species has been changed from that used by the original CRIv2-R5 mechanism in order to follow UKCA standards, the original name is also given. Species with 1 in the Strat column have been added to make the mechanism suitable for running in the stratosphere, species with 1 in the Aero column are only activated if running with GLOMAP-MODE.

Table S3.   Photolysis reactions in the CRI-Strat chemical mechanism. Reactions with 1 in the Strat column have been added to make the mechanism suitable for running in the stratosphere, reactions with 1 in the Aero column are only activated if running with GLOMAP-MODE. References for cross section data for reactions can be found in Telford et al. (2013). Reaction rates calculated online from the cross section data are multiplied by the scaling factor.

Table S4.   Bimolecular reactions in CRI-Strat chemical mechanism. Reactions with 1 in the Strat column have been added to make the mechanism suitable for running in the stratosphere, reactions with 1 in the Aero column are only activated if running with GLOMAP-MODE. Temperature dependent reaction rate coefficients k_0, a_0 and b_0 are given for the equation $k(T) = k_0(T/300)^{a_0}\exp(-b_0/T)$, where T is temperature in K.

Table S5.   Termolecular reactions in CRI-Strat chemical mechanism. Reactions with 1 in the Strat column have been added to make the mechanism suitable for running in the stratosphere, reactions with 1 in the Aero column are only activated if running with GLOMAP-MODE. Temperature and pressure dependent reaction rate coefficients k_1, a_1, b_1, k_2, a_2, b_2 and F are given for the equation $k(T) = (\frac{k_0(T)[M]}{1+k_0(T)[M]/k_i(T)})F_c^{(1+(log(k_0(T)/k_i))^2)^{-1}}$, where T is temperature in K; $[M]$ is the total number density in molecules cm^{-3}; $k_0 = k_1(T/300)^{a_1}\exp(-b_1/T)$ is the low pressure limit rate coefficient and $k_i = k_2(T/300)^{a_2}\exp(-b_2/T)$ is the infinite pressure limit rate coefficient. If $k_2 = 0$ then $k(T) = k_0(T)[M]$; if $k_1 = 0$ then $k(T) = k_i(T)$. The broadening term F_c is calculated from F as follows: if $0 > F < 1$ then $F_c = F$; if $F > 1$ then $F_c = \exp(-F/T)$; if $F = 0$ then the F_c term in the equation is ignored.

Table S6. Overview of tropospheric Ox burden, lifetime, ozone production efficiency (OPE), chemical production, chemical loss, deposition and inferred stratosphere to troposphere transfer. Values in brackets give fraction of total chemical production for the production terms and fraction of total losses ($L_{Ox} + D_{Ox}$) for the loss and deposition terms.

		StratTrop_orig	StratTrop_Ncon
O_3 burden (Tg)		**335.2**	**336.8**
O_x lifetime (days)		19.9	19.8
OPE ($mole_{O_3} mole_{NO_x}^{-1}$)		27.0	27.2
O_x production	**Total**	**5692**	**5725**
(Tg O_3 year^{-1})	$HO_2 + NO$	3832 (67.3%)	3853 (67.3%)
	$CH_3O_2 + NO$	1276 (22.4%)	1285 (22.5%)
	$R'O_2 + NO$	544 (9.6%)	545 (9.5%)
	Other[a]	40.2 (0.7%)	41.3 (0.7%)
O_x chemical Loss	**Total**	**5099**	**5128**
(Tg O_3 year^{-1})	$O(^1D) + H_2O$	2649 (43.0%)	2660 (42.9%)
	$HO_2 + O_3$	1586 (25.7%)	1596 (25.7%)
	$OH + O_3$	706 (11.5%)	714 (11.5%)
	$O_3 + Alkene$	96.4 (1.6%)	96.5 (1.6%)
	Other[b]	60.8 (1.0%)	61.5 (1.0%)
O_x Deposition	**Total**	**1061**	**1081**
	O_3 dry dep	892 (14.5%)	896 (14.4%)
	NO_y dep	170 (2.8%)	185 (3.0%)
Inferred STT (Tg O_3 year-1)		468	483

[a] O_x production channels are the sum of inorganic acid oxidation, $RONO_2$ oxidation and $RONO_2$ photolysis.

[b] "Other" O_x loss channels are the sum of $O(^3P) + O_3$, $O^3P + NO_2$, $N_2O_5 + H_2O$ and NO_3 chemical losses.

Table S7. Overview of air mass weighted OH concentration, CO burden and CO lifetime.

	StratTrop_orig	StratTrop_Ncon
[OH] (10^6 molecules cm^{-3})	1.33	1.34
CO burden (Tg)	301.2	300.2
CO lifetime (days)	38.8	38.6

Table S8. Overview of tropospheric oxidised nitrogen burdens (fraction of total NO_y in brackets), tropospheric oxidised nitrogen emission and deposition fluxes, stratosphere-troposphere transfer (STT) and NO_y lifetime in the troposphere (fraction of total NO_y deposition in brackets).

	StratTrop_orig	StratTrop_Ncon
NO_y Burden (Tg N)	0.993	1.018
NO_x Burden (Tg N)	0.151 (15.2%)	0.152 (14.9%)
NO_z Burden (Tg N)	0.842 (84.8%)	0.866 (85.1%)
$HONO_2$ Burden (Tg N)	0.491 (49.4%)	0.513 (50.4%)
Other inorganic NO_z (Tg N)	0.017 (1.7%)	0.018 (1.7%)
PANs (Tg N)	0.295 (29.7%)	0.296 (29.1%)
$RONO_2$ (Tg N)	0.039 (3.9%)	0.039 (3.9%)
Total NO_x Emissions (Tg N year^{-1})	61.5	61.5
Total NO_y Deposition (Tg N year^{-1})	58.3	62.9
Inferred STT (Tg N year^{-1})	-3.19	1.40
NO_x Dry deposition (Tg N year^{-1})	7.7 (13.2%)	7.70 (12.2%)
$HONO_2$ Wet deposition (Tg N year^{-1})	27.8 (47.7%)	30.1 (47.8%)
$HONO_2$ Dry deposition (Tg N year^{-1})	19.3 (33.1%)	21.6 (34.3%)
Other inorganic NO_z deposition (Tg N year^{-1})	0.97 (1.7%)	0.97 (1.6%)
PANs dry deposition (Tg N year^{-1})	1.28 (2.2%)	1.28 (2.0%)
$RONO_2$ deposition (Tg N year^{-1})	1.28 (2.2%)	1.30 (2.1%)